DESIGN REPORT
(T1706293) VER.5

KAGRA photon calibrator in X-end

Author:
C. Kozakai, Y. INOUE, Y. Chu, S. Haino, B. Hsieh, N. Kanda,
T.Shishido, T. Tomaru, T. Yamamoto, and T. Yokozawa
on behalf of the Calibration sub-group

KAGRA
Calibration subsystem

January 29, 2019

Abstract

KAGRA
Calibration subsystem

KAGRA photon calibrator in X-end

by C. Kozakai, Y. INOUE, Y. Chu, S. Haino, B. Hsieh, N. Kanda, T.Shishido, T. Tomaru, T. Yamamoto, and T. Yokozawa
on behalf of the Calibration sub-group

Accurate calibration of the output of the Gravitational Wave (GW) signal is crucial to determine the physics parameters of the sources. Also in the situation of global detector network, less relative bias between these detectors are important on the science of GW astronomy. LIGO, Virgo and KAGRA employ the photon calibrator that can calibrate the absolute displacement of the test mass by pushing the mirror surface with photon pressure. We employ three unique technologies for the KAGRA photon calibrator. (i)20W High power laser allows us the broadband calibration. (ii) We employ two optical follower servo for measuring the transfer function and mitigating the rotation effect of cryogenic suspension system. (iii) Beam position monitoring system is used for minimizing the elastic deformation. One of the serious systematic errors at high-frequency region is the elastic deformation of the mirror.

In this document, we report the current status of the KAGRA photon calibrator in X-end.

Acknowledgements

We cordially thank Prof. Rick Savage of LIGO Hanford Observatory who strongly encouraged and supported this work by sharing all the technical details and giving numerous critical comments and suggestions, together with LIGO calibration team, particularly, Dr. Evan Goetz, Dr. Kiwamu Izumi, Mr. Sudarshan Karki, Dr. Peter King, Dr. Jeff Kissel, Mr. Travis Sadecki, Mr. Darkhan Tuyenbayev and others. Virgo calibration team, particularly, Dr. Loic Rolland and others. We are greatful for the technical supports of KEK and Academia Sinica particularly by Ayako Hagiwara, Chih-hsun Lin, Yoshikazu Namai, Shinichi Terashima, and Ayako Ueda. We thank Dr. Tomotada Akutsu who helped us to fix the in-vacuum design. KAGRA project is supported by MEXT and JSPS in Japan as well as its collaborating institutes. YI and SH acknowledge the supports by Academia Sinica and MoST in Taiwan.

Contents

List of Figures

List of Tables

Chapter 1

Instruments descriptions

1.1 Layout of the Photon calibrator

The KAGRA photon calibrator is placed around EXA chamber, which is installed 36 m away from the end test mass (ETMX). We push the mirror surface with the modulated photon pressure directly. Figure 1.1 shows the layout of the KAGRA photon calibrator. The photon calibrator consists of transmitter module (Tx module), receiver module (Rx module), periscope, and telephoto camera module (TCam module). We place the 20 W laser in Tx module, whose wave length is 1047 nm. The 1064 nm laser is not used to avoid the coupling with main beams. The power of the laser is modulated by the optical follower servo (OFS). Details and performance of OFS is described in Chap. **??**. We split the beams in Tx module for pushing the drum head node points of the ETM due to elastic deformation. We transfer the beams to the ETM through the periscope. The periscope structures are placed into the EXA chamber. The beam is received by the Rx module. We place a 6 inches integrating sphere for the accurate measurement of the laser power and two quadrant photo detector (QPD) for the beam position monitor. We also measure the beam position on the ETM surface using the telephoto camera (TCam). The Tcam consists of the astronomical telescope, focuser, and high resolution digital camera. The specification summary of KAGRA photon calibrator is shown in Table. 1.1. Details of instruments are described in the following sections.

1.2 Placement of modules

The modules are placed around the EXA chamber. We need to pay attention to conflict with other components, such as optical lever stage, walls of the tunnel, doors of the chamber and working space. Figure. 1.2 shows the stay free regions around the EXA/EYA chamber. We need to avoid the red regions for mounting modules. All the modules meet our requirements. We make the anchor holes as shown in Fig. **??** and Fig. **??**. We employ the eagle anchor with 135 mm depth and M20.

TABLE 1.1: Specification summary of photon calibrator [1–3].

	KAGRA	**advanced LIGO**	**advanced Virgo**
Mirror material	Sapphire	Silica	Silica
Mirror mass	23 kg	40 kg	40 kg
Mirror diameter	220 mm	340 mm	350 mm
Mirror thickness	150 mm	200 mm	200 mm
Distance of Pcal from ETM	36 m	8 m	1.5 m
Pcal laser power	20 W	2W	3 W
Laser frequency	1047 nm	1047 nm	1047 nm
Incident angle	0.72 deg	8.75 deg	30 deg

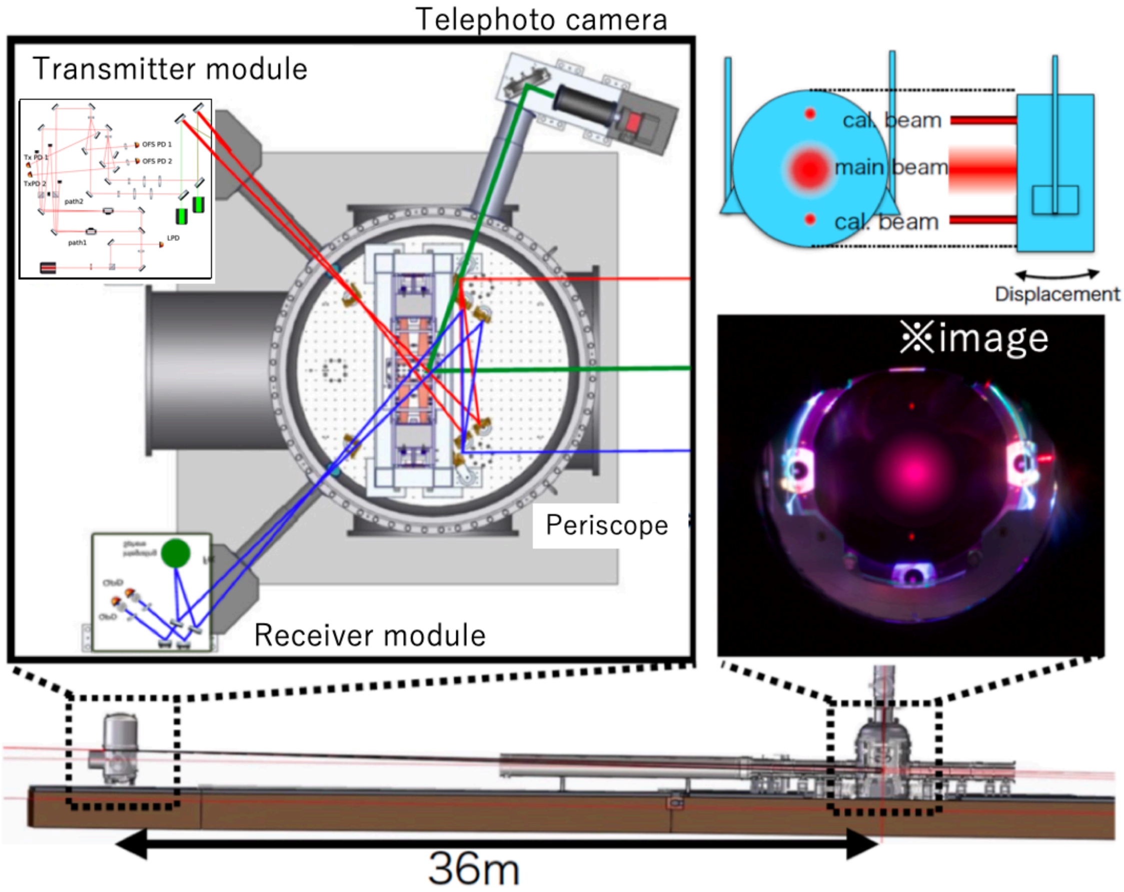

FIGURE 1.1: KAGRA photon calibrator. The calibration systems are placed around the EXA chamber. We mount the optical lever and optical baffle as well. The EXA chamber is placed at 36 m far from the ETMX. Transmitter module, receiver module and Tcam module are mounted on the ground by using eagle anchor (M20; SUS304). Each component is connected by aluminum duct to reduce the ghost of the image. We also mount the silica window for Tcam, Tx and Rx module.

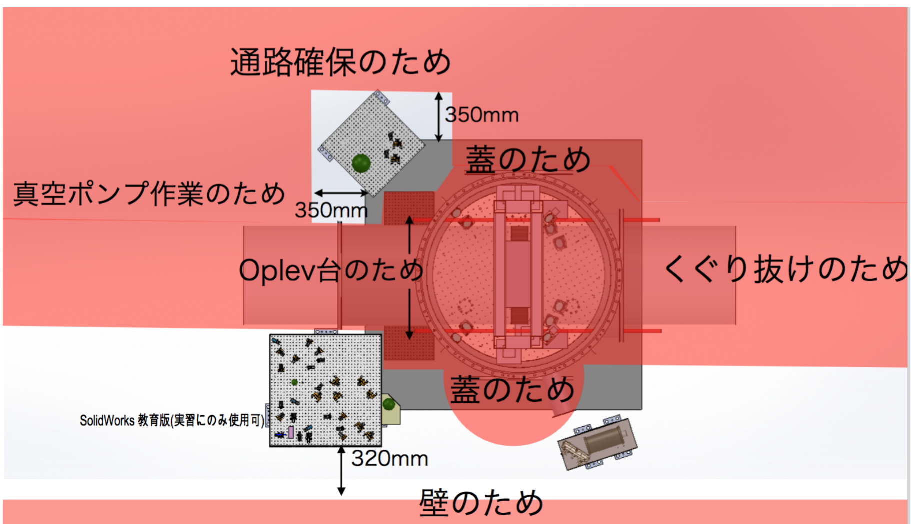

FIGURE 1.2: Stay free zone of the outside of the EXA/EYA chamber. All the components are placed at stay free region.

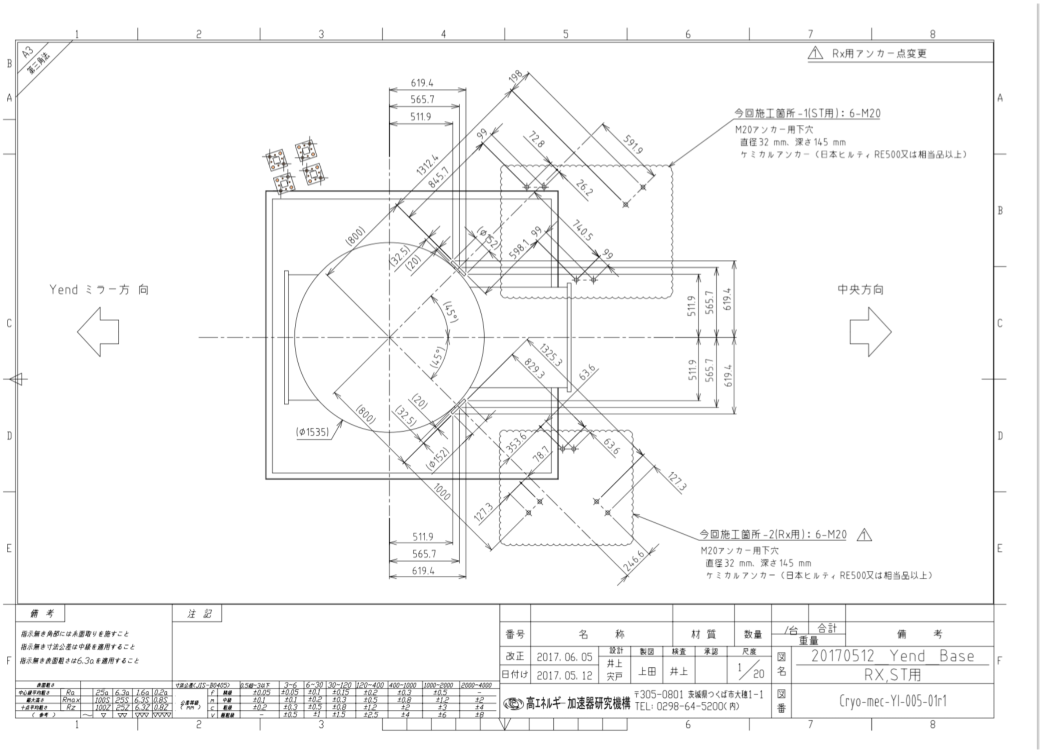

FIGURE 1.3: Drawing of Y-end anchor hole position.

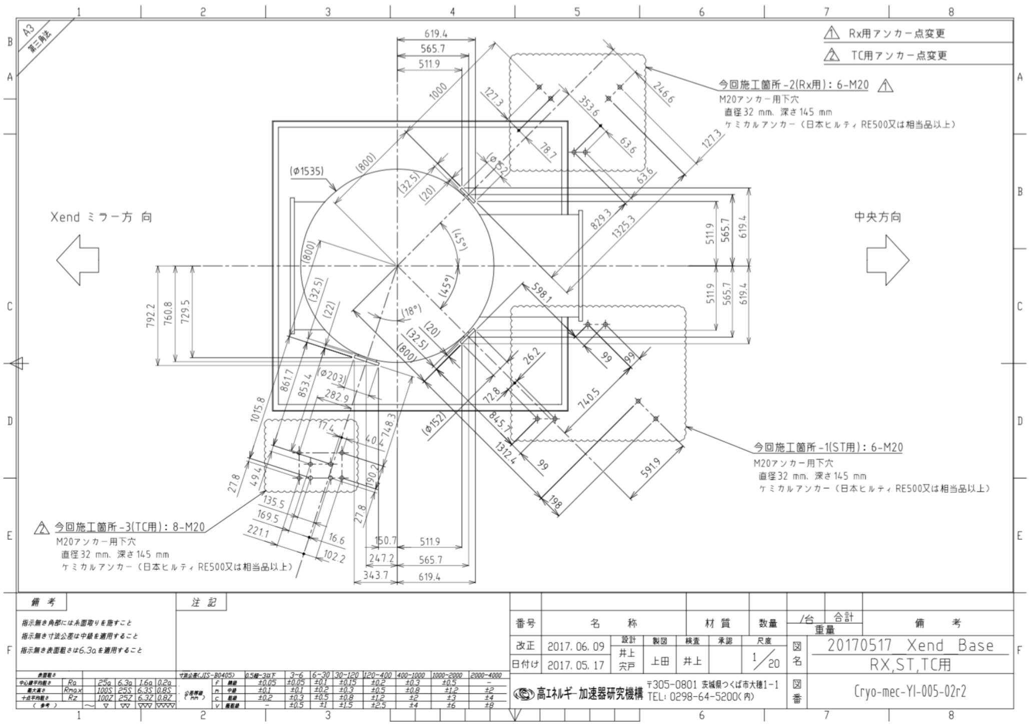

FIGURE 1.4: Drawing of X-end anchor position.

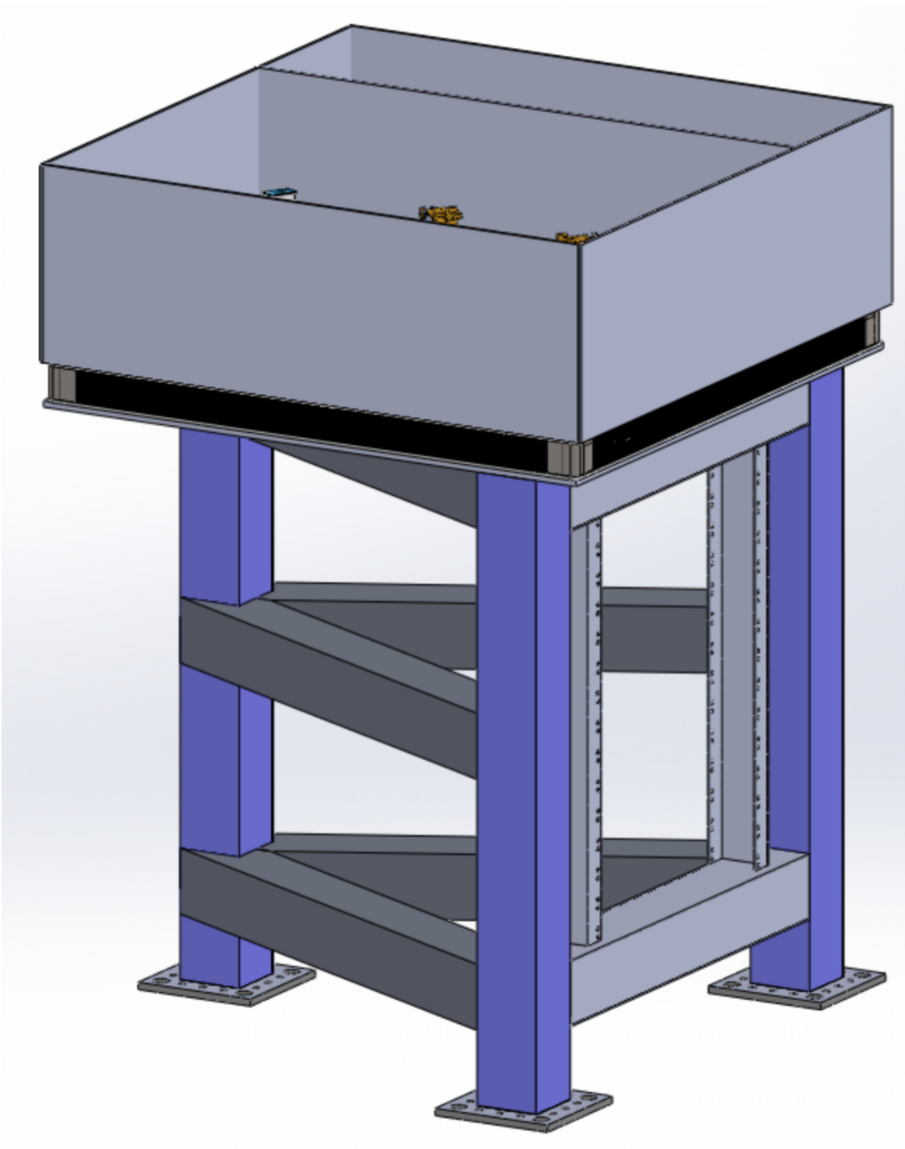

FIGURE 1.5: Transmitter module of the KAGRA Pcal. We place the optical table on the triangle table. The readout and control devices are housed into the legs of table.

1.3 Transmitter (Tx) module

The Tx module is placed at the side of the EXA chamber. Figure 1.5 shows the view of Transmitter module. All the optical components are mounted on the $900\ \mathrm{mm} \times 900\ \mathrm{mm}$ breadboard (B9090L; Thorlabs) [4]. The bread board is placed on the support structure. The electrical module for the control and readout are also hosed in the support structure as shown in Fig. **??**.

Figure 1.6 shows the optical layout of Tx module.

1.3.1 Yb fiber laser

We employ the CW fiber laser made by the LEA photonics as shown in Fig. 1.7. The maximum power is 20 W and the wave length is 1047 nm. The model number of the laser is CYFL-TERA-20-LP-1047-AM1-RG0-OM1-T305-C1 [5]. We use the isolator at the output port of fiber. The isolator is mounted on the stable aluminum block whose drawing is shown in Fig. 1.8. The maximum laser power of KAGRA Pcal is 10 times larger than that of LIGO. This

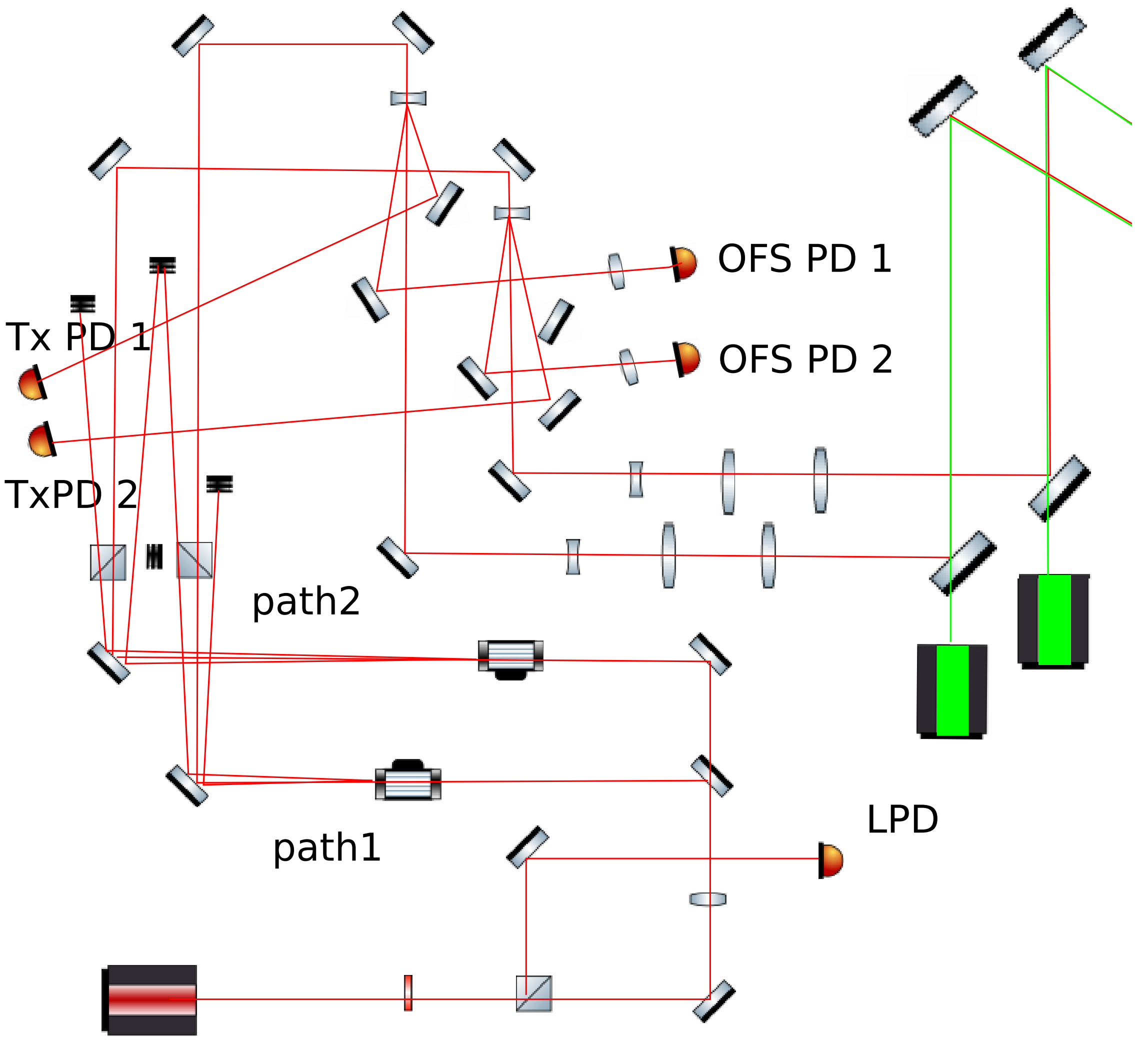

FIGURE 1.6: Optical layout of KAGRA photon calibrator. The laser power is modulated and controlled by the acousto-optic modulators (AOMs).

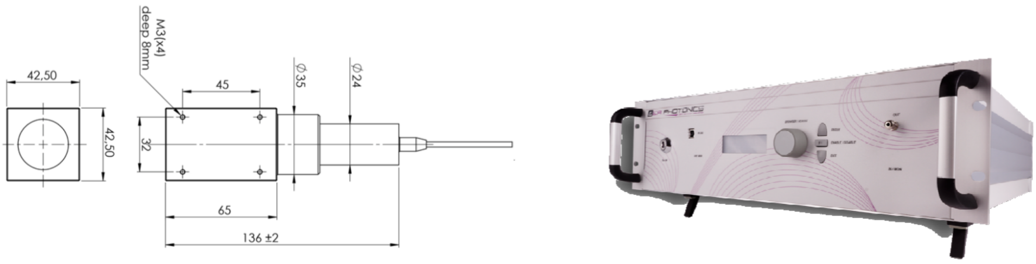

FIGURE 1.7: The fiber laser and drawing of isolator. The module is placed under the Tx module [5]. The maximum laser power is 20 W.

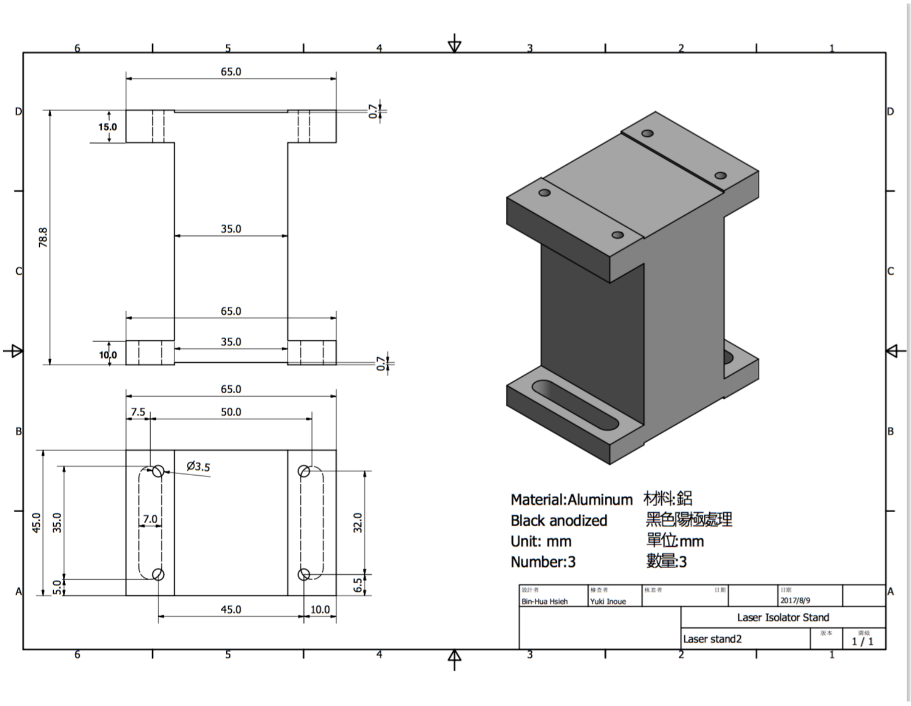

FIGURE 1.8: Isolator stand. The Isolator of the laser is mounted on the aluminum block.

is because we need the high power laser for the injection test and photon pressure actuator technique. The typical beam width of the laser is 0.25 mm when we mount the isolator. We summarize the specification of the laser as shown in Table 1.2.

The laser is operated with the active power control (APC) mode and the active current control (ACC) mode. We measured the output power of the laser using the power detector by changing the laser power and current. The measured power is shown in Fig. 1.9 and Fig. 1.10.

The property of the beam is measured with the beam profiler. The beam profiler can measure the beam width with two axis, X axis and Y axis. We estimate the beam waist of X and Y axis as shown in Fig. 1.11. The estimated beam width is listed in Table.1.3. Using the estimated value, we place the lens and make the focus point.

1.3.2 Beam shutter

We have to pay attention to safety for the operation of the high power laser. In order to dump the beam, we use the beam shutter made by Y. Inoue. We control the beam shutter on the MEDM as shown in Sec. **??**. We connect the laser shutter to interface chassis for controlling.

TABLE 1.2: Specification summary of Yb CW fiber Laser [5].

Characteristic	Typical value	Unit	Note
Operating central wavelength	1047	nm	± 1 nm
CW output power	20	W	
Output signal line-width	0.5	nm	FWHM
Output power stability	± 1	%RMS	Output power: 20 W
Output power tunability	10-100	%	
Optical polarization	Linier		
Polarization extinction ratio	15	dB	
Output fiber	PLMAFUD3460		Nufurn company
Output fiber length	2	m	
Beam diameter	0.5	mm	with isolator
Beam quality	1.1	M^2	
Control mode	Active current control, Active power control		
Supply voltage	84-264	V	AC 47 to 63 Hz
Power consumption	650	W	
Housing	448x451x132.5	mm	
Total weight	13	kg	
Cooling	Air cooled with fans		
Operating temperature	15-35		
Humidity	5-85	%	

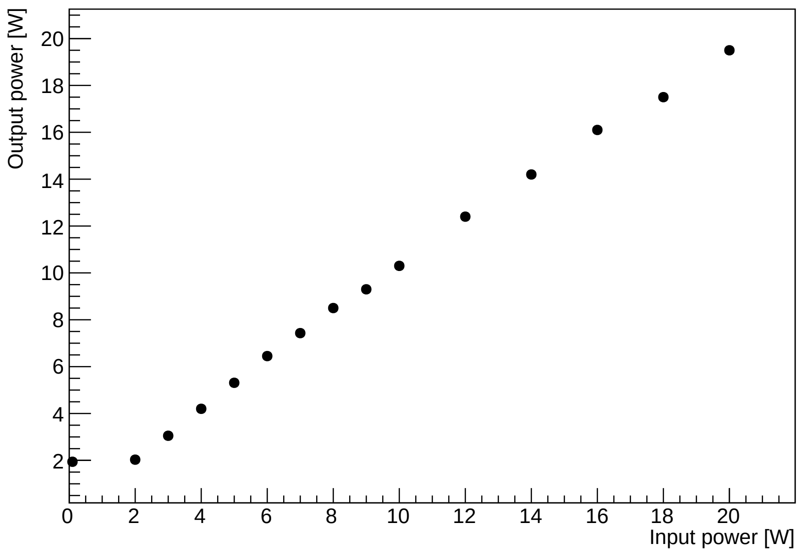

FIGURE 1.9: Output of active power control.

TABLE 1.3: Measured beam parameters.

Characteristic	Typical value	X	Y
Beam waist postion [mm]	0	3 ± 8	8 ± 9
Beam width [μm]	250	232 ± 3	238 ± 3

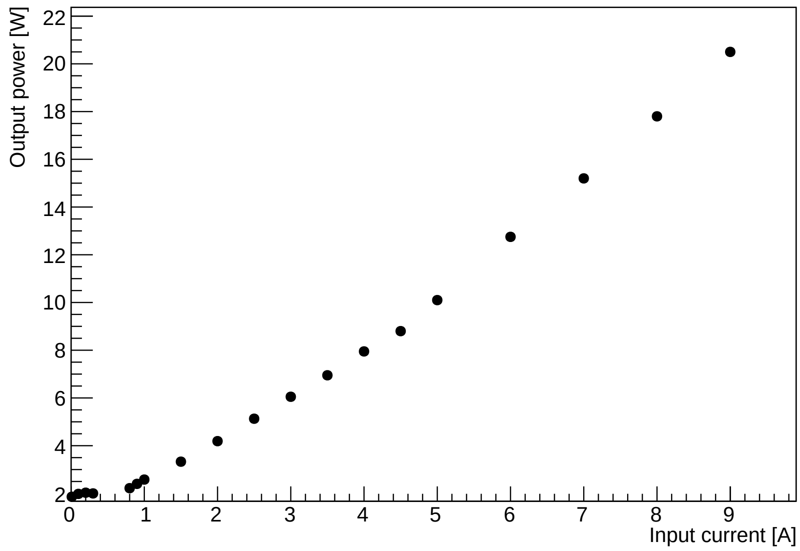

FIGURE 1.10: Result of active current control.

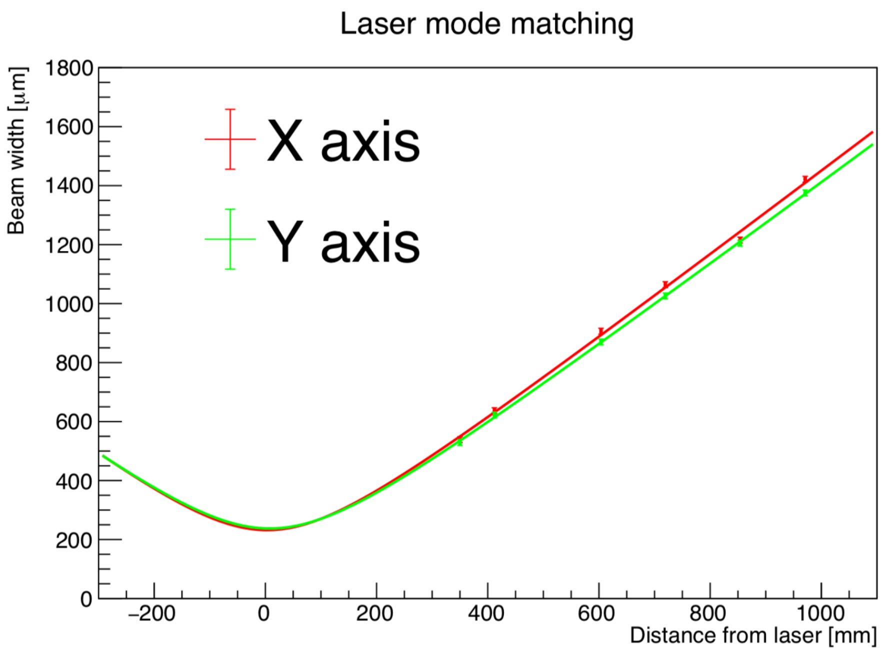

FIGURE 1.11: Result of beam measurement.

TABLE 1.4: Specification of HWP [6].

Characteristic	**Typical value**	**Unit**	**Note**
Waveplate Type	Quartz Waveplates		
Wavelength Range	1047	nm	
Retardance	$\lambda/2$		
Clear Aperture	85	%	of diameter
Reflection	0.25	%	
Retardance Tolerance	$\lambda/200$ to $\lambda/500$		at 23Degree C
Material	Crystal Quartz		
Surface Quality	10-5	scratch-dig	
Waveplate Diameter	12.7	mm	

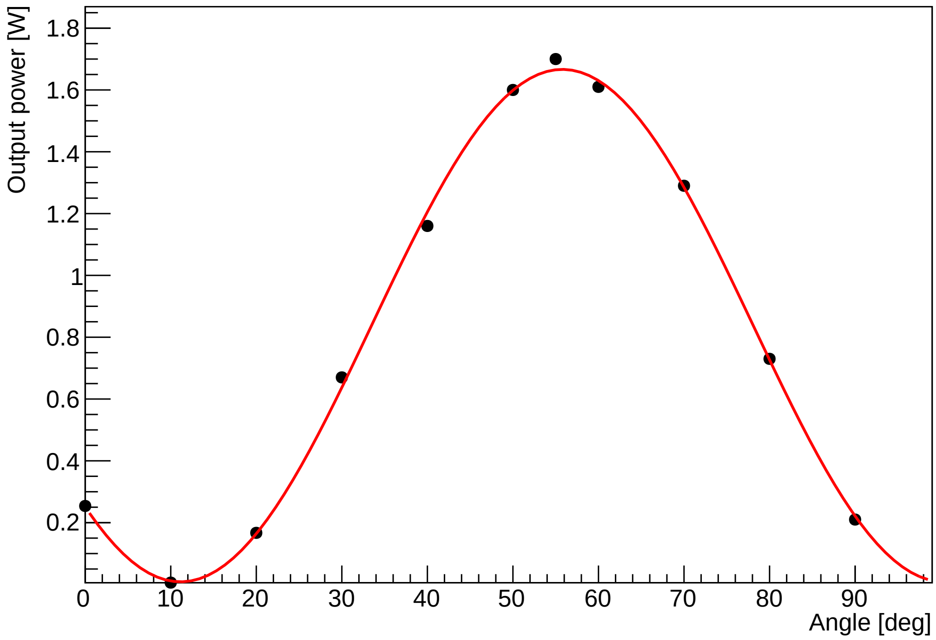

FIGURE 1.12: The measured polarization response of HWP.

1.3.3 Zeroth order half wave plate

To control the polarization angle of the incident beam, we employ the zeroth order half wave plate (HWP) made by the CVI laser optics [6]. The model number of the HWP is QWPO-1047-05-2-R10 whose diameter is 12.7 mm. The HWP is mounted on the rotation mount made by Thorlabs. The thickness are optimized at 1047 nm. The specification of the HWP is listed in Table 1.4. We measure the polarization response using detector as shown in Fig. 1.12.

1.3.4 Polarizer

We place two polarizers to define the polarization angle accurately. This is because that the power of the laser is modulated by acousto-optic modulator (AOM) whose performance depends on the incident polarization angle. One polarizer is placed behind HWP. Another one is placed after AOM. The polarizer is made by Karl-Lambrecht [7]. We purchased TFPC12-1047 that is optimized at 1047 nm.

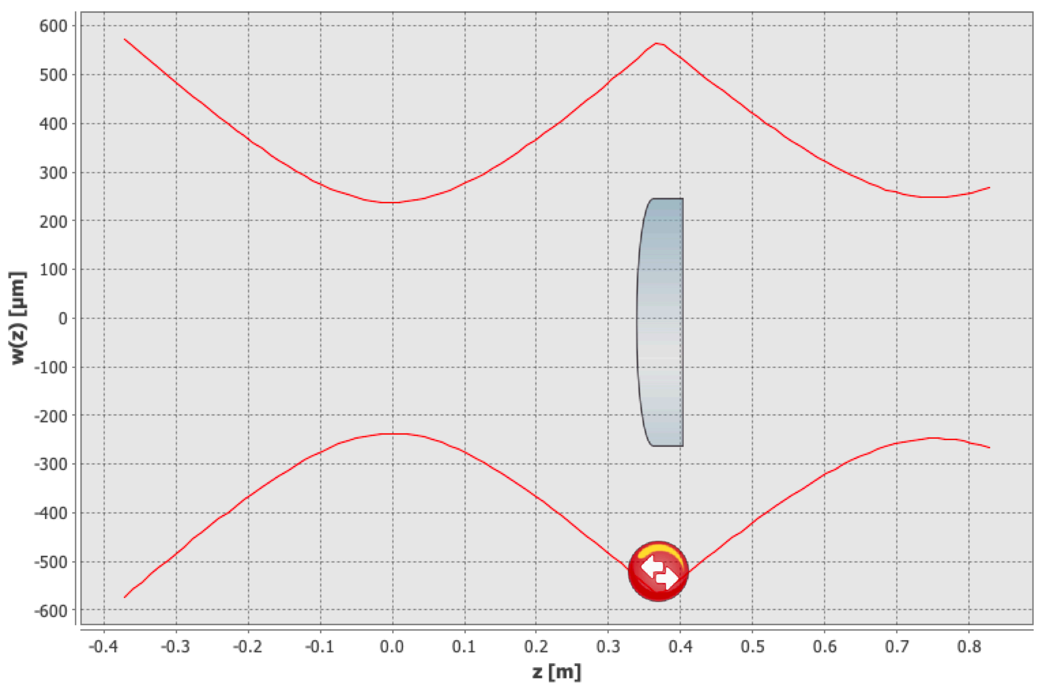

FIGURE 1.13: Result of mode matching calculation from faber laser to AOM focus using JamMt [8].

1.3.5 Lens

We have done mode matching simulation using JamMt [8]. We assumed laser beam to be gaussian distribution. We need to place the focus of the laser at the AOM. Thus, we decide the optimal position and focal length of the 1 inch lens (LTx1), where the assumed beam waist of the fiber laser and AOM are 0.25 mm, respectively. The estimated beam spot size and lens position are shown in Fig. 1.13.

Furthermore, we place three lenses for placing the focus at the surface of the ETM. We employ the combination of 1 inch negative lens and 2 inch positive lenses. The Gaussian beam can describe the following relation:

$$w(z) = \omega_0 \sqrt{1 + \left(\frac{\lambda z}{\pi \omega_0^2}\right)^2}, \tag{1.1}$$

where λ is wavelength of the laser, w_0 is beam waist, z is direction from the focus. We estimate the minimum differential beam spot by changing beam waist because it make the alignment easier. The minimum beam spot is written by

$$\left.\frac{dw(z)}{dw_0}\right|_{z=36\ \mathrm{m}} = 0. \tag{1.2}$$

The estimated beam spot size is 5.0 mm at Tx module with 3.5 mm beam waist as shown in Fig. 1.14.

The parameters of the simulation results are listed in Table. 1.5. All lenses are made by CVI laser optics [6]. The material of lenses are fused silica. The AR coating are placed on both surface.

1.3.6 Mirror

We employ fourteen 1 inch mirrors and four 2 inch mirrors. The 1 inch mirror is made by CVI laser optics [6]. They place the HR coating on the surface of mirror. On the other hand, we use the HR coating on the fused silica disc of 2 inch in diameter. The coating and polishing

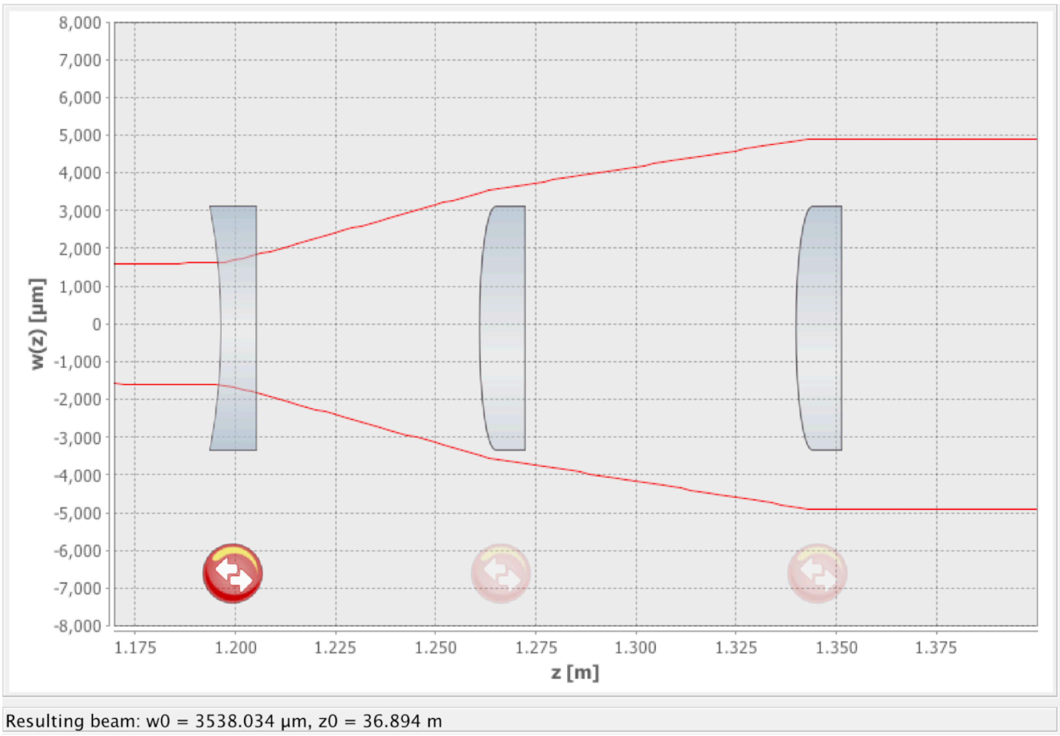

FIGURE 1.14: Result of mode matching calculation from AOM to ETMX focus using JamMt [8]. $z = 0$ is at AOM.

TABLE 1.5: Specification of lenses [6].

Lens number	part number	Diameter [mm]	Focal length (mm)	z (mm)	w_0 (mm)
LTx1	PLCX250UV (CVI laser optics)	25.4	286.457	371	0.25
LTx2	PLCC50UV (CVI laser optics)	25.4	-57.38	1940	-
LTx3	PLCX250UV (CVI laser optics)	50.8	286.326	2010, 2080	3.5

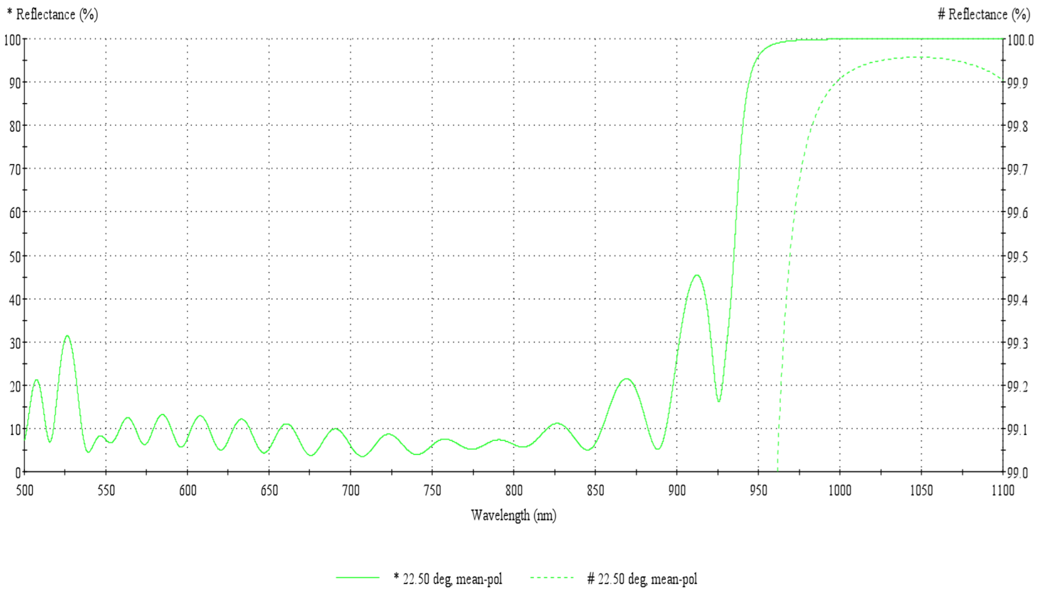

FIGURE 1.15: The simulated HR coating on the fused silica mirror for 22.5 degree of incident angle [9].

the fused silica are made by Sigma-koki corporation [9]. The reflectances of the mirrors with 22.5 deg and 45 deg are shown in Fig. 1.15 and Fig. 1.16. The reflectance of the HR coating depends on the incident angle and the polarization angle. We labeled mirrors as shown in Fig. 1.6. The specification of mirrors are summarized in Table. 1.6. All mirror is aligned with optical mirror mount made by Newport company.

1.3.7 Optical mount with Pico-motor

The uncertainty of the beam position on the ETMX is one of the largest systematic errors. To control the beam position, we employ Pico-motor for changing mirror angle (see Fig. 1.6). The pico-motor is made by New port [10], whose part number is 8301NF. We mount the Pico-motor on the mirror mount of MTxU10 and MTxL10. We control the Pico-moter using beam monitoring chassis.

1.3.8 Beam splitter

To reduce the elastic deformation, we separate the beam with the beam splitter made by CVI laser optics. The part number of beam splitter is BS1-1064-50-1012-45P. The diameter of the beam splitter is 1 inch. Table 1.7 shows the separation ratio of beam splitter. The incident angle of the laser to the BS is adjusted to get same transmittance and reflectance efficiency.

1.3.9 Twin AOM

We employ the AOM as laser power modulator for making calibration line, which made by ISOMET companiy [11]. We make the two focus points using beam splitter and place the AOMs. The requirement of the beam width is 250 μm. We connect the AOM and optical follower servo for reducing the noise and higher harmonics. The detail of optical follower servo is described in Chap. **??**. The part number of AOM is M1080-T80L-M. The specification is shown in Table 1.8.

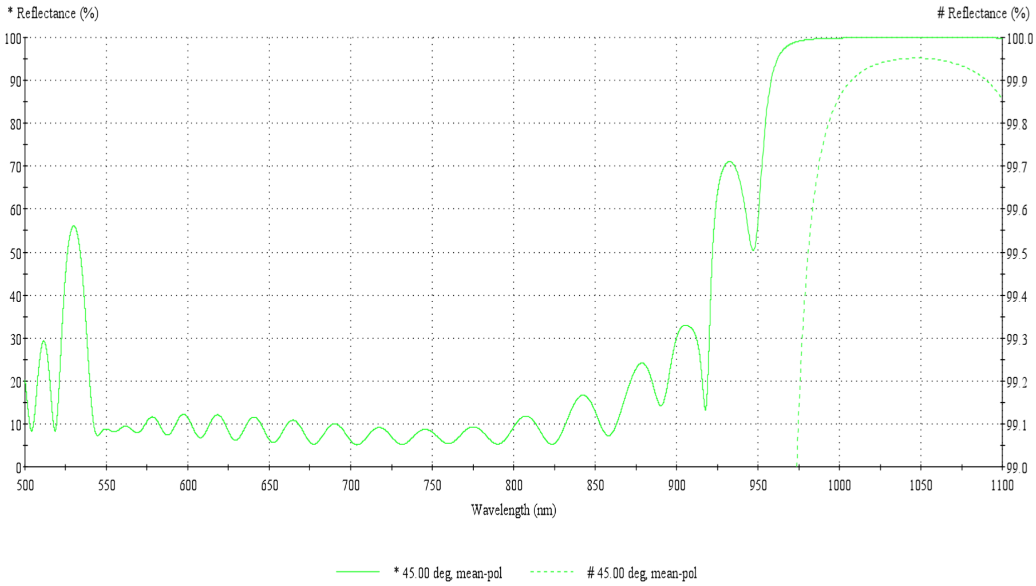

FIGURE 1.16: The simulated HR coating on the fused silica mirror for 45 degree of incident angle [9].

TABLE 1.6: Specification of Mirrors.

Mirror number	part number	Diameter [mm]	Incident angle (design value)	Polarization
MTx1	Y1S-1025-45 (CVI)	25.4	45	P
MTx2	Y1S-1025-45 (CVI)	25.4	45	P
MTxU3	Y1S-1025-45 (CVI)	25.4	45	P
MTxL3	Y1S-1025-45 (CVI)	25.4	45	P
MTxU4	Y1S-1025-45 (CVI)	25.4	45	P
MTxL4	Y1S-1025-45 (CVI)	25.4	45	P
MTxU5	Y1S-1025-45 (CVI)	25.4	45	P
MTxL5	Y1S-1025-45 (CVI)	25.4	45	P
MTxU6	Y1S-1025-45 (CVI)	25.4	25	P
MTxL6	Y1S-1025-45 (CVI)	25.4	25	P
MTxU7	Y1S-1025-45 (CVI)	25.4	25	P
MTxL7	Y1S-1025-45 (CVI)	25.4	25	P
MTxU8	Y1S-1025-45 (CVI)	25.4	45	P
MTxL8	Y1S-1025-45 (CVI)	25.4	45	P
MTxU9	Sigma-koki(TBC)	50.8	45	P
MTxL9	Sigma-koki(TBC)	50.8	45	P
MTxU10	Sigma-koki(TBC)	50.8	20.9	P
MTxL10	Sigma-koki(TBC)	50.8	24.1	P

TABLE 1.7: Specification of beam splitter [6].

Characteristic	Typical value	Unit	Note
Beamsplitter Type	Laser Line Plate Beamsplitters		
Beamsplitter Shape	Round		
Wavelength Range	800	nm	
Bevel/Chamfer	0.35 mm $\times$ 45 Degree		
Wedge Angle Tolerance	5	arcmin	
Coating Material	Laser Line Dielectric		
Angle of Incidence	45	Degree	
Clear Aperture	85	%	
Substrate/Material	Fused Silica		
Surface Flatness	$\lambda/10$		
Surface Quality	10-5	scratch-dig	
Beamsplitter Diameter	50.8	mm	
Beamsplitter Thickness	6.35 mm		
Thickness Tolerance	± 0.25 mm		

TABLE 1.8: Specification of AOM [11].

Characteristic	Typical value	Unit	Note
Spectral Range	$0.36 > 1.5$	μm	
AR Wavelengths	700 -900 or 1064	nm	
Interaction Medium	Tellurium Dioxide (TeO2)		
Acoustic Velocity	4.2	$\mathrm{m}/\mu\mathrm{s}$	
Centre Frequency (Fc)	80	MHz	
RF Bandwidth	30	MHz	
Input Impedance	50	Ω	
VSWR	<1.5:1 @ Fc		
Clear Aperture	3.5	mm	
Active aperture	1.5	mm	
Static Insertion Loss Reflectivity	<3	%	
Laser Polarization	Any		
DC Contrast Ratio	1000:1 min		
Cooling	conduction		
Optical Power	20	W	
Beam Diameter	0.5	mm	
Optical Rise Time	77	ns	
Deflection efficiency	>85	%	Pol.: Perpendicular to Base
RF power	2.8	W	1064nm
Bragg angle	10.5	mrad	1064nm

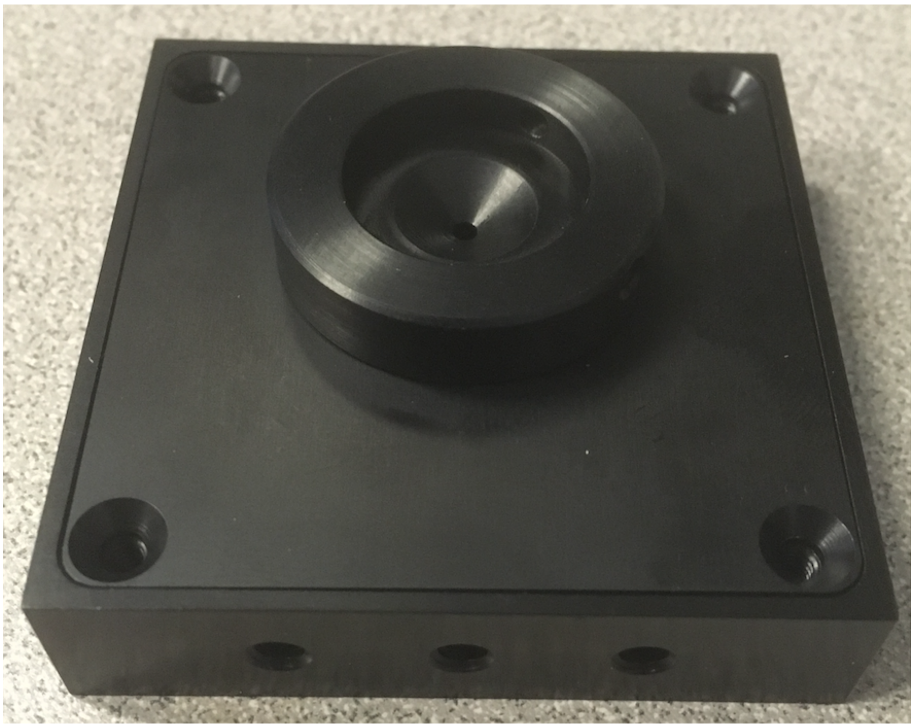

FIGURE 1.17: Developed photo detector for KAGRA Pcal.

TABLE 1.9: Specification of InGaAs detector.

Charactaristic	Typical value	Unit	Note
Dark Current	25	nA	
Peak Wavelength	1550	nm	
Responsivity	0.75	A/W	
Breakdown Voltage	50	V	
Capacitance	200	pF	

1.3.10 Photo detector

To detect the laser power, we use the photo detector. We place the photodetector at the working standard, Optical follower servo PDs, Integrating spheres in Tx and Rx module. We developed the photo detector as shown in Fig. 1.17. We employ the InGaAs photo diode for absolute power measurement. The InGaAs diode is placed on the circuit board. The beam is collimated for the power detection reasonably.

Cover

The cover is designed by the LIGO Pcal group. We make the detector cover in Academia Sinica, Institute of Physics. Figure 1.17 shows the machined detector covers. We housed the circuit board into the cover coated by the black anodized aluminum (MIL-A-8625F, TYPEII,CLASS2).

InGaAs detector

We employ the C30665GH, which is large area InGaAs PIN photodiode with diameter of 3.0 mm with a flat glass window. The C30665GH provides high quantum efficiency from 800 nm to 1700 nm. This detector is fabricated by Excelitas [12]. The specification of detector is shown in Table. 1.9.

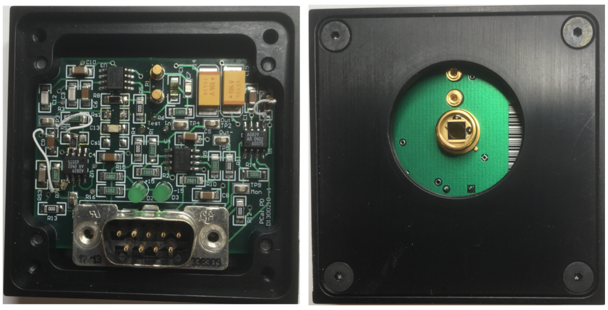

FIGURE 1.18: The picture of photo detector. The diameter of photo detector is 3 mm. We control the incident power by changing diameter of the collimator and resistance of trans impedance amplifier

TABLE 1.10: Parameter of amplifier.

Detector	**Rt** $[k\Omega]$	**Ct** $[pF]$	**Rg** $[k\Omega]$
OFS PD	75	5.6	2.0
LPD	10	5.6	2
TxPD	10	5.6	2
RxPD	100	5.6	2

Electrical Circuit

We newly improved the electrical circuit of the photon detector as shown in Fig. 1.18. The electrical circuit is housed in the aluminum cover. We place the photo detector at the behind of the electrical circuit. The circuit consists of 4 layer. We change the differential gain by changing the register and capacitor of the circuit. The electrical circuit are shown in Fig. 1.19. The circuit gain can control the Rg (R8) and Rt (R7) by the purpose. We use this electrical circuit as Integrating sphere of Tx module, OFS, Integrating sphere of Rx module, and Working standard KAGRA. Each parameter is listed in Table 1.10.

1.3.11 Beam sampler

To make the feedback loop, we need to pick up the laser output using the beam sampler. LIGO uses the polarization beam sampler, which is significantly sensitive to incident polarization angle. To avoid this difficulty, we plan to employ the diffractive beam sampler. Diffractive beam sampler is used to monitor high power lasers where optical losses and wavefront distortions of the transmitted beam need to be kept to a minimum. In most applications, most of the incident light must continue forward, "unaffected," in the "zero order" while a small amount of the beam is diffracted into a higher order, providing a "sample" of the beam. We will use the SA-220-1047-Y-A made by HOLO/OR Ltd [].

The operational principle is quite straightforward. From a collimated input beam, the output beams exit from Diffractive Optical Element (DOE) with a separation angle that is determined during the design of the DOE. The beams separation is designed for far-field so that as the beams continue to propagate after DOE. A Diffractive Beam Sampler allows the high power beam (zero order) to propagate along the optical axis, but produces two side beams with low energy. These two sample beams are located to the left and right of the main beam (-1 and +1 orders).

1.3.12 Green laser

We employ the 532 nm green semi-conductor laser for alignment. We place the green laser behind the MTxU9 and MTxL9.

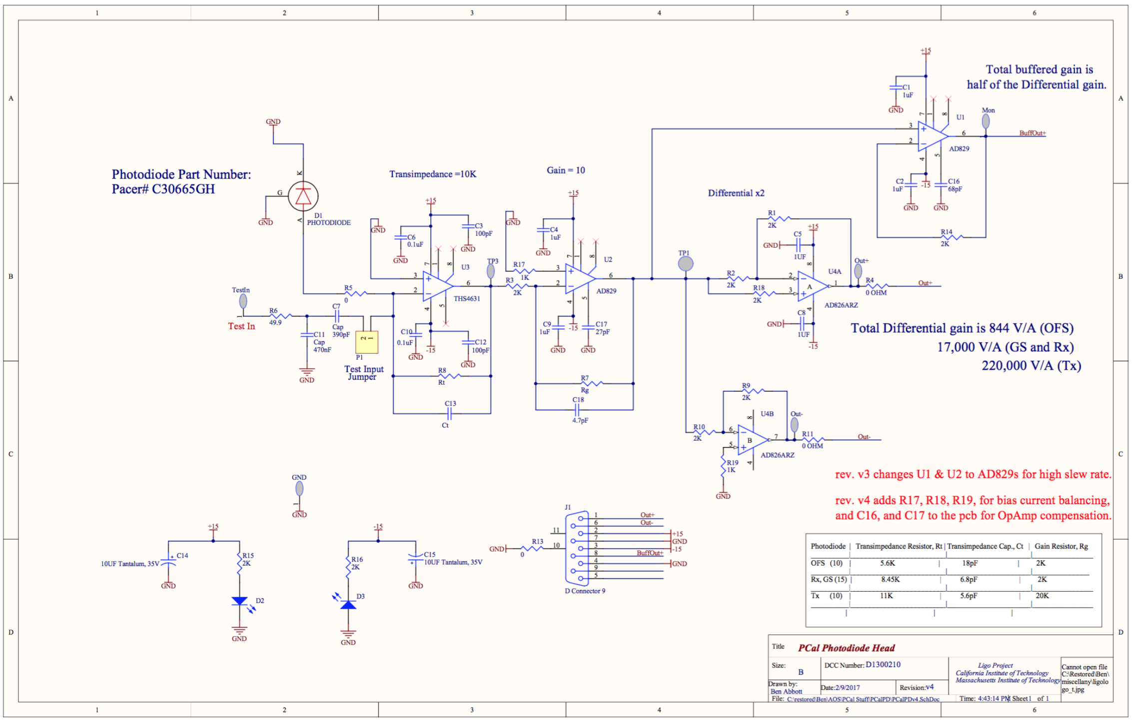

FIGURE 1.19: Circuit of photo detector designed by LIGO (D1300210-v4).

1.3.13 2 inch integrating sphere

The 2 inches integrating sphere is used for the absolute power measurement of the laser. We receive the separated laser beam at beam sampler. We mount the photo detector (TxPD) at the port of the integrating sphere. The integrating sphere is made by the Lab sphere. The inner surface of the integrating sphere in mounted on the Spectralon [13]. The measurement of the absolute power is described in Chap. **??**

1.3.14 Structure

The breadboard is placed on the support structure as shown in Fig 1.20. The material of this structure is SUS 306. This structure houses electrical devices, such as driver of the fiber laser, electronics of optical follower servo, driver of AOM, readout electronics of photo detectors, network hubs, and beam position control system. There are also DC power supply for AOM driver and binary input and Dsub connector interchanging box.

1.4 Receiver module

The purpose of the receiver module is to measure the absolute power of laser and beam position control. All the components are mounted on the optical bench 600×600 mm optical table (B6030L, Tourlabs) [4]. The optical bench is mounted on the structure. To accomplish the purpose, we introduce QPD and 6 inch integrating sphere. The accuracy of beam position and absolute power are corresponding to the systematic errors.

1.4.1 6 inch Integrating sphere

The 6 inches integrating sphere is used for absolute power measurement of the laser. We receive the laser beam from two paths. To receive the power perfectly, we need a large diameter hole of integrating sphere at least 2 inch. We use for the 2 inch hole integrating sphere. We mounted the photo detector at the top of the port. Details of the photo detector is explained in Sec. 1.3.10.

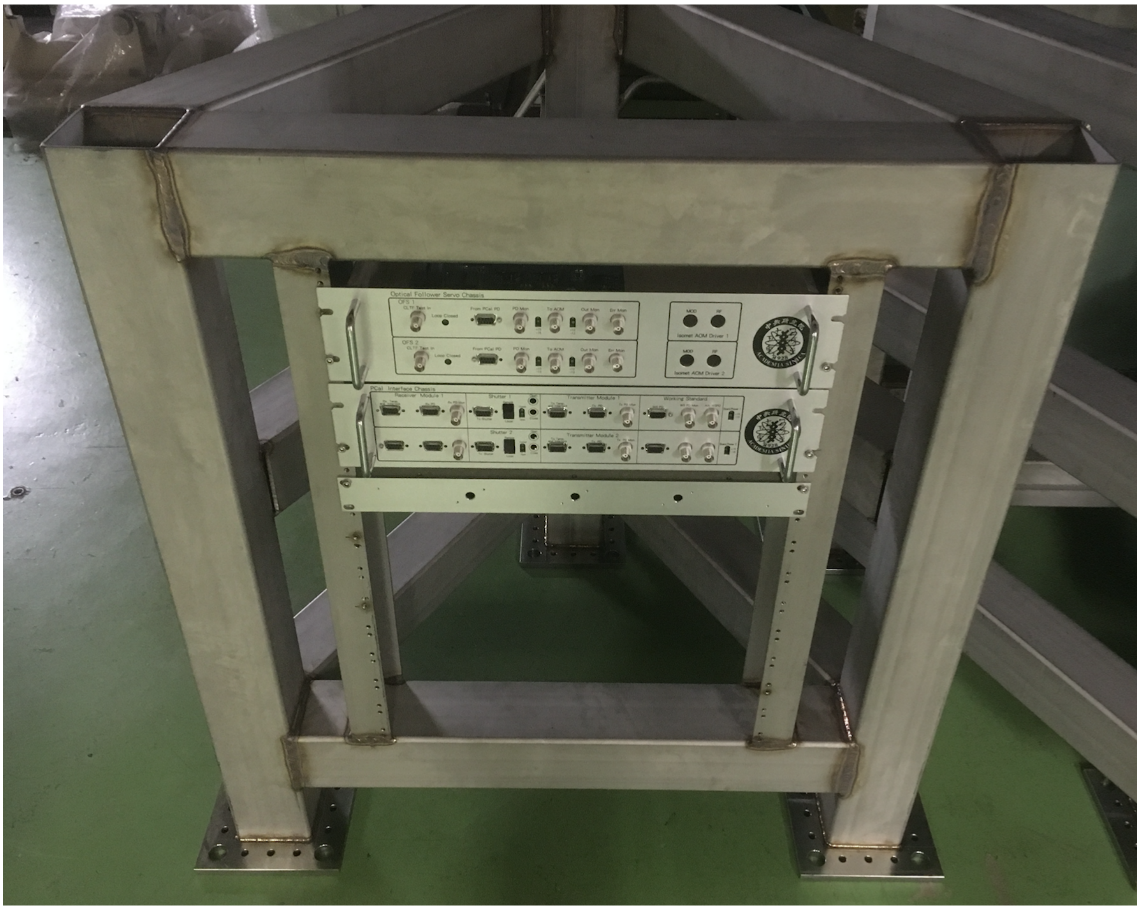

FIGURE 1.20: Structure of Tx module.

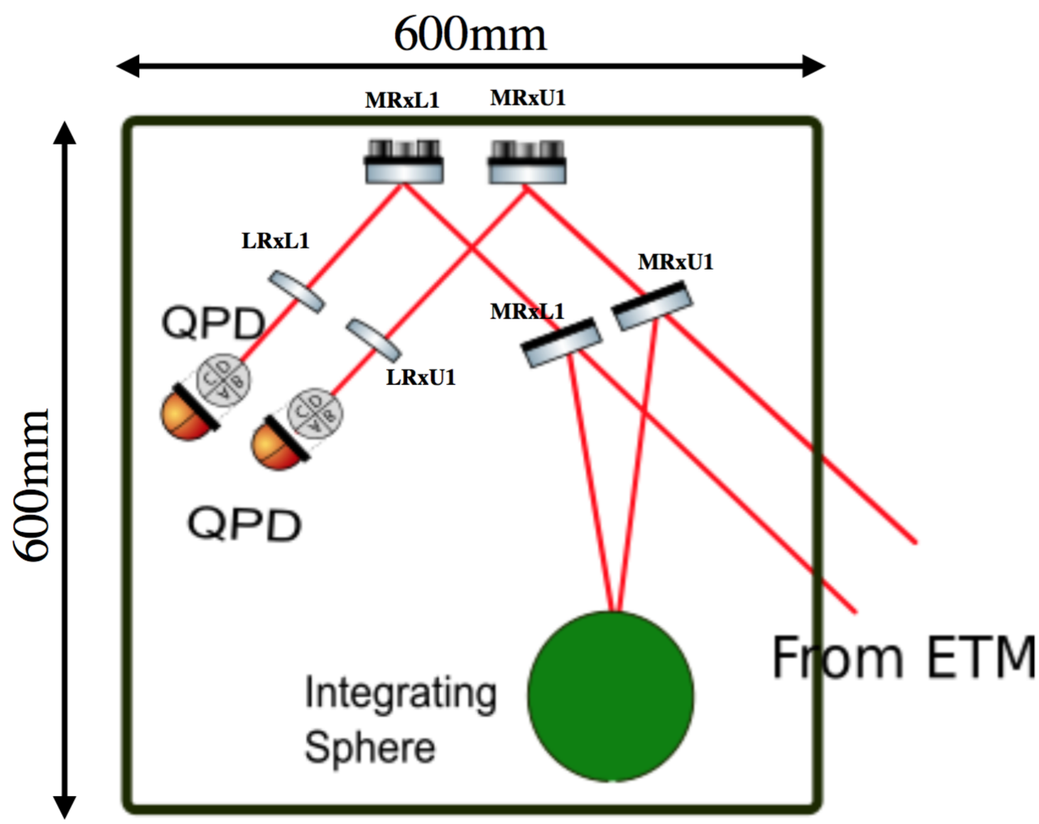

FIGURE 1.21: Optical layout of receiver module. We mounted QPD for monitoring beam position drift. Total power of the laser is measured by the integrating sphere.

TABLE 1.11: Specification of Mirrors in Rx module in design value.

Mirror number	part number	Diameter [mm]	Incident angle	Polarization
MRxU1	Sigma-koki	76.2	47deg	P
MRxL1	Sigma-koki	76.2	43deg	P
MRxU2	Sigma-koki	76.2	45deg	P
MRxL2	Sigma-koki	76.2	45deg	P

1.4.2 Mirror

We employ four 3 inch mirrors. We place the HR coating made by Siguma-koki as shown in Fig. 1.16 and 1.15. For two mirrors, we make the AR coating on the back surface to pick up the beams. The specification of the mirrors are listed in Table 1.11.

1.5 Electronics

Please refer the test procedure.

Bibliography

[1] L. Rolland, F. Marion, and B. Mours, "Conceptual design of advanced virgo photon calibration", Virgo TDS **0013A**, 15 (2015).

[2] S. Karki et al., "The Advanced LIGO Photon Calibrators", Rev. Sci. Instrum. **87**, 114503 (2016).

[3] M. Ando, "Observation Scenario Paper", JGW **G1706116** (2017).

[4] Thorlabs,

[5] Keopsys,

[6] C. laser optics,

[7] Polarizer, "Tfpc12-1047",

[8] JamMt,

[9] Sigma-koki,

[10] Newport,

[11] I. laser optics,

[12] Excelitas,

[13] Labsphere, "Spectralon",

[14] Cosmotech,

[15] ANSYS®Academic Research, Release **17.1** (2016).

[16] D810,

[17] Skywatcher, "Maksutov-cassegrain",

[18] E. MEDM,

[19] S. Hild et al., "Photon pressure induced test mass deformation in gravitational-wave detectors", Class. Quant. Grav. **24**, 5681–5688 (2007).

[20] E. Goetz et al., "Precise calibration of LIGO test mass actuators using photon radiation pressure", Class. Quant. Grav. **26**, 245011 (2009).

[21] H. P. Daveloza, M Afrin Badhan, M Diaz, K Kawabe, P. N. Konverski, M Landry, and R. L. Savage, "Controlling calibration errors in gravitational-wave detectors by precise location of calibration forces", Journal of Physics: Conference Series **363**, 012007 (2012).

[22] COMSOL®Multiphysics, Release **5.2a** (2016).

[23] S. Kuck, "Responsivity of detectors for radiant power of lasers, final report, edited by stefan kuck", EUROMET Comparison Project **156**, EUROMET.PR–S2 (2009).

[24] B. P. Abbott et al., "Calibration of the Advanced LIGO detectors for the discovery of the binary black-hole merger GW150914", arXiv **1602**, 03845 (2016).

[25] D. Tuyenbayev et al., "Improving LIGO calibration accuracy by tracking and compensating for slow temporal variations", Class. Quant. Grav. **34**, 015002 (2017).

[26] T. Tanaka and H. Tagoshi, "The Use of new coordinates for the template space in hierarchical search for gravitational waves from inspiraling binaries", Phys. Rev. **D62**, 082001 (2000).